Gysi *et al. BMC Bioinformatics* (2018) 19:392
https://doi.org/10.1186/s12859-018-2351-7

BMC Bioinformatics

SOFTWARE Open Access

wTO: an R package for computing weighted topological overlap and a consensus network with integrated visualization tool

Deisy Morselli Gysi[1,2*], Andre Voigt[3], Tiago de Miranda Fragoso[4], Eivind Almaas[3,5] and Katja Nowick[6]

Abstract

Background: Network analyses, such as of gene co-expression networks, metabolic networks and ecological networks have become a central approach for the systems-level study of biological data. Several software packages exist for generating and analyzing such networks, either from correlation scores or the absolute value of a transformed score called weighted topological overlap (*wTO*). However, since gene regulatory processes can up- or down-regulate genes, it is of great interest to explicitly consider both positive and negative correlations when constructing a gene co-expression network.

Results: Here, we present an `R` package for calculating the weighted topological overlap (*wTO*), that, in contrast to existing packages, explicitly addresses the sign of the *wTO* values, and is thus especially valuable for the analysis of gene regulatory networks. The package includes the calculation of *p*-values (raw and adjusted) for each pairwise gene score. Our package also allows the calculation of networks from time series (without replicates). Since networks from independent datasets (biological repeats or related studies) are not the same due to technical and biological noise in the data, we additionally, incorporated a novel method for calculating a consensus network (*CN*) from two or more networks into our `R` package. To graphically inspect the resulting networks, the `R` package contains a visualization tool, which allows for the direct network manipulation and access of node and link information. When testing the package on a standard laptop computer, we can conduct all calculations for systems of more than 20,000 genes in under two hours. We compare our new wTO package to state of art packages and demonstrate the application of the wTO and CN functions using 3 independently derived datasets from healthy human pre-frontal cortex samples. To showcase an example for the time series application we utilized a metagenomics data set.

Conclusion: In this work, we developed a software package that allows the computation of *wTO* networks, *CN*s and a visualization tool in the `R` statistical environment. It is publicly available on CRAN repositories under the GPL—2 Open Source License (https://cran.r-project.org/web/packages/wTO/).

Keywords: Co-expression network, Network, Expression, R package, Software, Consensus Network, wTO, Meta analysis, Co-occurrence network, Metagenomics

*Correspondence: deisy@bioinf.uni-leipzig.de
[1]Department of Computer Science, Interdisciplinary Center of Bioinformatics, University of Leipzig, Haertelstrasse 16-18, 04109 Leipzig, Germany
[2]Swarm Intelligence and Complex Systems Group, Faculty of Mathematics and Computer Science, University of Leipzig, Augustusplatz 10, 04109 Leipzig, Germany
Full list of author information is available at the end of the article

Background

Recent applications of complex network analysis methods have provided important new knowledge of the functioning and interactions of genes at the systems level [1–4]. Within the area of biological network analyses, co-expression networks have received much attention [5, 6]. For the co-expression networks, a pair of nodes are typically connected by a link if the genes they represent show a significantly correlated expression pattern. In the network, this link may be represented as a binary relationship, where 1 = "presence" and 0 = "absence" of the link, or alternatively, the link may have a numeric value (often called weight). The magnitude of the weight is typically interpreted as representing the strength of a gene-pair relationship, and the sign as indicative of the type of associated gene interaction: positive if the genes are co-regulated, negative if they are oppositely controlled [7].

In many implementations of network analyses, we may primarily be interested in an *a priori* defined subset of genes with a specific set of properties. Examples include transcription factors (TFs), genes with known orthologs in a set of organisms of interest, or disease associated genes [8, 9]. For these situations, oftentimes the choice is made to only take into account direct interactions between the gene-subset of interest, instead of including the full set of correlations. A major drawback with such an approach, is that relevant information contained in interaction patterns among excluded genes that would affect network topology and link strength values, is not incorporated in the network. The loss of such information is not only undesirable, but may also lead to biased results.

When analyzing networks in which the links have non-binary weights, the method of weighted topological (*wTO*) network analysis [10] has been found very useful. In a *wTO*-analysis, a new link-weight for a pair of connected nodes is determined through an averaging process that accounts for *all* common network neighbors [10]. Thus, *wTO* is a method that *implicitly* includes correlations among nodes that are going to be exempt from further analysis. The *wTO* method [10–12] can be used to determine the overlap among classes of transcripts, for example TFs and non-coding RNAs (ncRNAs). The resulting *wTO* network provides a more robust representation of the connections and interactions among the node-set of interest than a simple correlation network analysis focused only on the node-set of interest [13].

The packages `WGCNA` [14, 15] and `ARACNe` [16, 17] are widely used for weighted gene co-expression network analysis studies. The former provides functions for the calculation of the adjacency matrix for all pairs of genes as the n-th power of absolute correlations, resulting in an unsigned network. Network modules can be defined with this package by unsupervised clustering. The latter uses the mutual information (MI) of the expression in order to build the networks. These methods have received much attention in the literature [7, 18].

Previously, Nowick and collaborators [13] developed a mathematical method to calculate the *wTO* for a set of nodes that explicitly takes into account both positive and negative correlations. This version of the *wTO*-measure is especially valuable for investigating networks, in which it matters whether an interaction is activating or inhibiting/repressing. For instance, in gene regulatory networks the effect of a transcription factor or a ncRNA on its target genes can be activating or repressing. In metabolic networks, the increase of a substance can lead to an increase or decrease of another substance. Or in ecological networks, species interactions can be positive or negative, for instance in symbiotic or predator-prey relationships. In such cases, a distinction between positive and negative correlations for the calculation of the *wTO* is necessary and using the absolute correlations would falsify the biological insights. This *wTO*-calculation methodology is implemented in the `R` package presented here. In order to avoid confusion, we will refer to the method for calculating a pair-wise link score as *wTO* and to the package as `wTO`.

When analyzing similar datasets, e.g. from a repeated experiment or independent studies on a similar subject, the resulting networks are usually different [19]. These differences may arise from several sources: (A) technical differences, such as the platform on which the expression data was measured, the facility where data was collected and prepared, or how data was processed. (B) Another cause may be biological differences from confounding factors, such as sex, age, and geographic origin of the individuals measured. It is thus desirable to obtain an integrated network that considers all independently derived networks as biological replicates and systematically identifies their commonalities. We developed a novel method to compute the network that captures all this information; we call this the consensus network (*CN*).

Here, we present `wTO`, an `R` package that is capable of computing both signed and unsigned *wTO* networks as well as the *CN*, thus providing methods for assigning *p*-values to each link. The package also comes with an integrated tool to visualize the resulting networks and allows for nine different methods for network clustering to aid in module identification. The workflow of the package is shown in Fig. 1.

We compare our method to other state of art methods. To exemplify the usage of our package, we show here results from the calculation of *wTO* and *CN* networks from three independent genome-wide expression studies of healthy human pre-frontal cortex samples and an analysis of a time-series dataset from a metagenomics study.

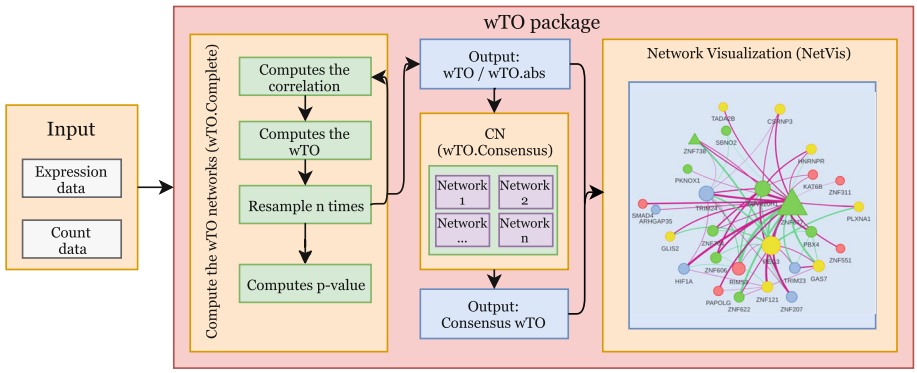

Fig. 1 The `wTO` package workflow. Gray boxes refer to inputs, red boxes refer to content of the `wTO` package, yellow boxes are functions included in the package, blue boxes are outputs of those functions, and green boxes refer to methods internal to the package. Our package can deal with multiple kinds of data, for example RNA-seq counts or normalized values, microarray expression data, abundance data coming from metagenomic studies, and many more. All input data should be pre-processed with the quality control and normalization methods recommended for each respective type of data. The function `wTO.Complete` calculates the *wTO* values, as many times as desired. As output, the user will obtain an object containing the signed and absolute *wTO* values for each pair of nodes, *p*-values and p_{adj}-values for multiple testing. This output can be used for the construction of a *CN* from independent networks using the function `wTO.Consensus`. Outputs from the *wTO* and *CN* networks can be used as an input for `NetVis`, which is an integrated tool for plotting networks. As an interactive tool it also allows the user to modify the network

Implementation

Input data

Our package can handle a wide range of input data. Data can be discrete or continuous values. We recommend performing all commonly used steps for quality control and normalization before passing on the data to our package. For RNA-Seq data, our package can handle normalized quantification, for example RPKM (Reads Per Kilobase Million), FPKM (Fragments Per Kilobase Million), and TPM (Transcripts Per Kilobase Million). For microarray data, rma or mas5 values can be used. If our package is used with metagenomics data, for instance for analyzing co-occurrence networks, we recommend the abundance data to be normalized per day/sample.

Weighted topological overlap calculation

For a system of N nodes (e.g. genes or species), we define the adjacency matrix $A = [a_{i,j}]$ based on correlations between a pair of nodes i and j as

$$a_{i,j} = \begin{cases} \rho_{i,j} & i \neq j \\ 0 & i = j. \end{cases} \quad (1)$$

with $\rho_{i,j}$ being a correlation measure. Assuming that nodes i and j represent a sub-set of factors (e.g genes) of particular interest selected from the N nodes, we calculate the weighted topological overlap (*wTO* [13], $\omega_{i,j}$) between node i and node j as

$$\omega_{i,j} = \frac{\sum_{u=1}^{N} a_{i,u}a_{u,j} + a_{i,j}}{\min\left(k_i, k_j\right) + 1 - \left|a_{i,j}\right|}, \quad (2)$$

where

$$k_i = \sum_{j=1}^{N} \left|a_{i,j}\right|. \quad (3)$$

Note that, this expression explicitly includes both positive and negative correlations, and thus allows for $\omega_{i,j}$ to take both positive and negative values. Other software packages calculating the $\omega_{i,j}$ have implemented definitions of the *wTO* method that do not allow for negative values [14], making this version valuable for gene regulatory network analysis. The `wTO` package also calculates the unsigned network, and for that, it takes as an input the absolute values of the correlation.

Since Eq. (2) explicitly allows $a_{i,j} \leqslant 0$, we need to be aware of the limits of this expression. Consider three nodes i, j and u, and assume that $a_{ij} \leqslant 0$. All the terms in the numerator of Eq. (2) will be negative if $a_{iu}a_{uj} \leqslant 0$ for all nodes u. However, if $a_{iu}a_{uj} > 0$, then at least some contributions to the sum will cancel out. The same rationale applies for the case of $a_{ij} \geq 0$.

To systematically assess the potential effect of term cancellation in Eq. (2), we calculate the absolute weighted topological overlap, $|\omega|$ which uses the absolute value of the correlations ($a_{i,j} = |a_{i,j}|$) as input for Eq. (2). In this case, the sign of the correlation is excluded from the analysis and only the magnitude of the link-strength is taken into account. Consequently, by generating a scatter plot of the signed and unsigned weights, it is possible to assess at which $\omega_{i,j}$-values term cancellations start affecting the results. Thus, for *wTO* values of interest, the closer the plot of ω vs. $|\omega|$ is to $y = |x|$, the better.

However, by just computing the *wTO* network we do not avoid all spurious correlations. A way to detect them is to

compute a probability of each one of the link scores being zero using the hypothesis test

$$\begin{cases} H_0 : \omega_{ij} = 0 \\ H_a : \omega_{ij} \neq 0 \end{cases}, \quad (4)$$

of the null hypothesis (H_0) of no association against the two-sided alternative (H_a) of non-zero association. This can be computed by using bootstrap [20] or permutation resampling methods [13]. In the former, one resamples individuals, thus approximating the weights' empirical distribution and calculating the probability that an observed weight is sufficiently distant from zero. In the latter, one operates under the null hypothesis of no dependence among genes and permutes the gene labels, obtaining the weights' distribution under the null hypothesis, which is rejected if the observed weight is sufficiently extreme. We define δ as the maximal distance between the $\omega_{i,j}$ calculated with each bootstrap and the $\omega_{i,j}$ of the real dataset. This means that, the smaller δ is, the stronger is our confidence in a particular $\omega_{i,j}$. By default, δ is set to 0.2.

One advantage of the `wTO` package is its application to analyze and make networks out of time-series data. Therefore, we are interested in the implementation of blocked bootstrap resampling [20] that can be used for temporal data without sample replicates for each time point. This type of resampling is necessary once there are two correlation components in those samples: The correlation inside the factors of each sample and the correlation across the time of different samples. For this situation, the use of a lag is required. Lags are particularly helpful in time-series analyses as autocorrelations are often present: a tendency of consecutive values to be correlated. An important benefit of the presence of autocorrelations is that we may be able to identify patterns inside a time-series, such as seasonality (patterns that repeat themselves at a periodic frequency). Therefore, the lag can be chosen using a partial correlation of the time per sample. This is followed by calculating the *wTO* for a time series where the observations are not independent of each other.

A method for determining a consensus network

Berto and collaborators [19] described a consensus network based on gene-expression data from primates' frontal lobes by applying a Wilcoxon test on the links. Our proposed methodology allows the use of two or more datasets, each generating different (and significant) *wTO* values, to be combined into a single *CN*. Our approach has the advantage of penalizing links with opposite signs. According to the same rationale, links with the same sign among the multiple *wTO* networks, will have their $CN_{i,j}$ values closer to the largest $\omega_{i,j}$ of a link among the k networks. Our first step is to remove nodes that do not exist in all networks. Consequently, if a node is absent in at least one network, we are not able to compute a consensus of the links that belong to that node. It is particularly important not to associate factors that were not measured in a particular condition.

In order to obtain a single integrated network derived from multiple independent *wTO* networks, we calculate a *CN* using the following approach:

If we have $k = 1, \ldots, n$ replicated networks (note that n means the index of the networks, not the exponent of α nor ω), then we define the consensus network $\text{wTO}_{\text{CN}} = \left[\Omega_{i,j}\right]$ as

$$\Omega_{ij} = \sum_{k=1}^{n} \alpha_{ij}^{k} \omega_{ij}^{k}, \quad (5)$$

where

$$\alpha_{ij}^{k} = \frac{\left|\omega_{ij}^{k}\right|}{\sum_{k=1}^{n} \left|\omega_{ij}^{k}\right|}. \quad (6)$$

A threshold can be used to remove links with $\Omega_{i,j}$ values close to zero, thus should not be included in the consensus network. To join networks that were generated with the proposed wTO method into the consensus network, the p-values are combined using the Fisher's method.

Results and discussion

The representation of interactions between a set of nodes by the *wTO* method [10–12] takes into account the overall commonality of all the links a node has, instead of basing the analysis only on calculating raw correlations among the nodes. It thus provides a more comprehensive understanding of how two nodes are related. Therefore, it is expected that a *wTO* network contains more robust information about the connections among nodes than what would result from simply taking direct correlations into account [11, 13]. The *wTO* can be computed based on a similarity matrix, where the link weights are calculated using Pearson's product moment correlation coefficient or the Spearman Rank correlation. The first one measures the linear relationship between two genes. Note that, the Pearson's correlation coefficient is sensitive to extreme values, and therefore it can exaggerate or underreport the strength of a relationship. The Spearman Rank Correlation is recommended when data is monotonically correlated, skewed or ordinal, and it is less sensitive to extreme outliers than the Pearson coefficient [21–24].

Package functions

The function `wTO` calculates the weights for all links according to Eq. (2) between a set of nodes for a given input data set. If the user is not interested in the resampling option, one may simply run this `wTO` function.

To test whether the calculated `wTO` is different from random expectation and to decide on a suitable threshold value for including link weights, we implemented the

function `wTO.Complete`. Here, the *wTO* is calculated a number of times, *n* specified by the user, by using either the 1) Bootstrapping (`method_resampling = "Bootstrap"`), or (`method_resampling = "BlockBootstrap"`) for time series data or 2) Permuting the expression values for each individual (`method_resampling = "Reshuffle"`) [13]. The user may specify the correlation method that this function should use, Pearson correlation is the default choice.

Because bootstrapping and permutation tests can be computationally expensive, the `wTO.Complete` can also run in parallel over multiple cores to reduce the wall clock time. For running in parallel, the user may specify a given number of *k* computer threads to be used in the calculations. To implement the parallel function, we used the `R` package `parallel` [25].

The execution of the `wTO.Complete` function returns two outputs; a diagnosis set of plots and a list consisting of the following three objects:

- `$Correlation` is a data.table containing the Pearson or Spearman correlations between all the nodes, not only the set of interest. The *wTO* links for the set of nodes of interest are based on these correlations. The default of this output is set to `FALSE`.
- `$wTO` is a data.table containing the nodes, the *wTO* values (signed and unsigned), the *p*-values and the adjusted *p*-values computed using both signed and unsigned correlations.
- `$Quantile` is a table containing the quantiles for the empirical distribution, computed using the bootstrap and the quantiles for the real data: 0.1%, 2.5%, 10%, 90%, 97.5% and 99.9%. Those empirical values can be used as a threshold for the *wTO* values, when it is not desired to visualize low *wTO* scores.

The set of plots indicate the quality of the resample: the closer the density of the resampled data is to the real data, the better. Another generated plot is the scatter plot of the $\omega_{i,j}$ vs $|\omega_{i,j}|$, as previously discussed. The scatter plot of *p*-values against the $\omega_{i,j}$ and $|\omega_{i,j}|$ is also plotted along with suggested threshold values that are the empirical quantiles.

Computing of the *CN* is done using the function `wTO.Consensus`. This function allows the user to give a list of networks in the format of data.frames with: Node 1, Node 2, the link weight and the *p*-value. The output is a data.table containing the two nodes' names and the consensus weight, and the combined *p*-value. This allows the user to filter out the links that were not significant in part of the networks. A visual representation of the Consensus Network methodology is shown in Fig. 2. The thicker the link between two nodes is, the stronger the correlation between them. The signs are represented by the colors blue and orange, respectively. If a link has different signs in the networks, the strength of the link in the *CN* is close to zero. When all links agree to the same

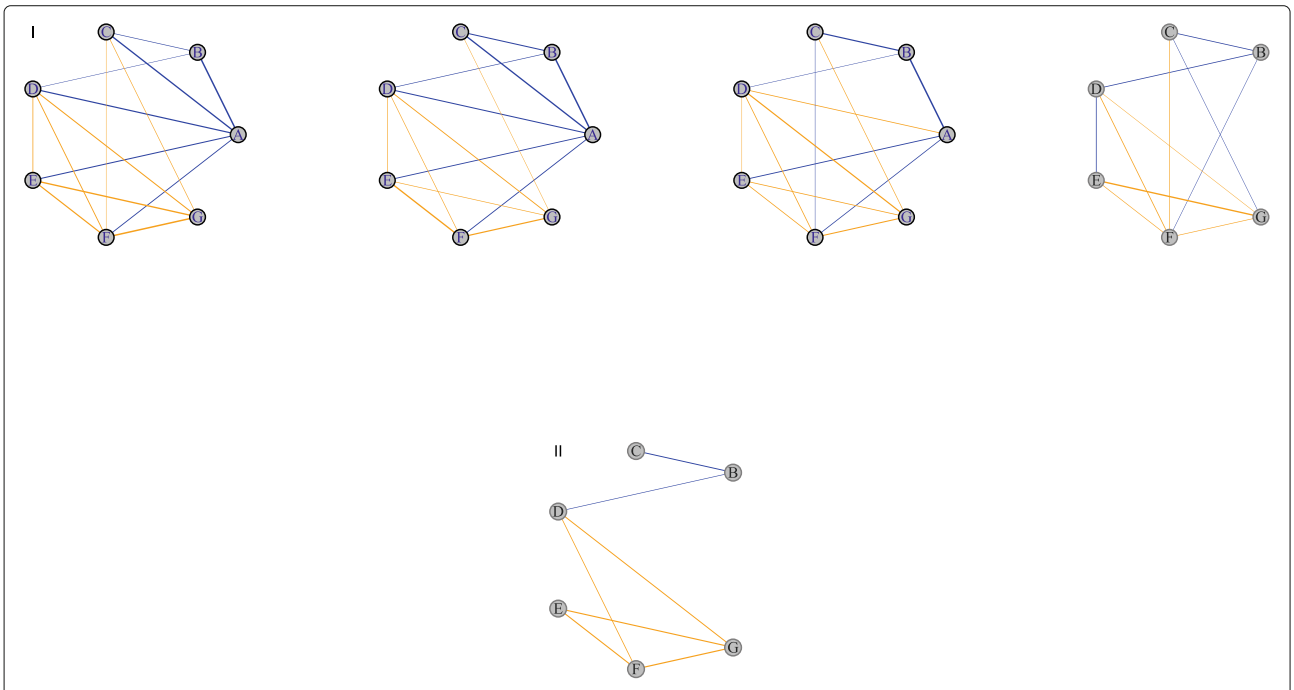

Fig. 2 A schematic example of the *CN* method: Panel **I** shows four independent networks to be combined into one *CN*. Note that the rightmost network does not include the 'A' node. Blue links indicate negative sign, while orange, positive. The *CN* can be seen on Panel **II**. Note that the missing node from Panel **I** is not present in the *CN*. Also, only links that are constant in their sign among networks are present in the final network. For example, the link between D and E is removed since it has a different signal in the last network

value or show little deviation, the strength of the resulting *CN* value is closer to the determined |*maximum*| value. If a node is absent in at least one network, it is removed.

The output data.frames (from both, `wTO.Complete` and `wTO.Consensus`) can be easily exported using the function `export.wTO`. This allows, for instance, to pass on the results of our package to Cytoscape [26] for further analysis.

Our `R` package also includes options to visualize the resulting networks. The function `NetVis` generates an interactive graph using as input a list of links and their corresponding weights. The analysis functions `wTO.Complete` and `wTO.Consensus` both generate network data-structures (edge list) that can be visualized with this function. The user needs to choose a relevant *wTO*-threshold (the quantiles resulting from the bootstrap), or *p*-value cut-off, to select the set of links to be plotted. Additionally, the user may choose a layout for the network visualization from those available in the `igraph` [27] package. By default, the *wTO*-threshold value is set to 0.5, and the network layout-style is set to `layout_nicely`. To avoid false positives, we recommend to filter the data according to the desired significance *p*-value and to choose the *wTO*-threshold according to the computed empirical quantiles. The size of the nodes is relative to their degree. Our package further includes an option for `MakeCluster` from the nodes; if allowed, nodes are colored according to the cluster they belong to. The user can choose the method to create the clusters.

One important difference between our package and the `WGCNA` package, is that we only use significant links for cluster (modules) network representation instead of the full set of co-expressions, as in the `WGCNA` package. The width of a link is relative to the $wTO_{i,j}$, and its color is respective to its sign (if a signed network was calculated). Nodes can have different shapes, allowing for labeling nodes of different classes, for example target genes or protein coding and non-protein coding genes. Furthermore, the user may also zoom in and out of the network visualization, drag nodes and links, edit nodes and links, and export the image as html or png. The package provides example datasets and an example of nodes of interest as well.

Algorithm compute time with varying system size

Normally, when running the *wTO*, the interest lies on a subset of nodes of interest. In Fig. 3 we show the runtime for different network sizes, and different proportions of nodes of interest. When running the *wTO* for all expressed genes coding for transcription factors (TFs) being the genes of interest, we have around 14% of nodes of interest. Using a standard laptop computer, it's possible to compute the *wTO* for a full network with 20,000 nodes in 20 miliseconds per link. This shows that it is quite feasible to compute the full *wTO* for a realistic gene expression network.

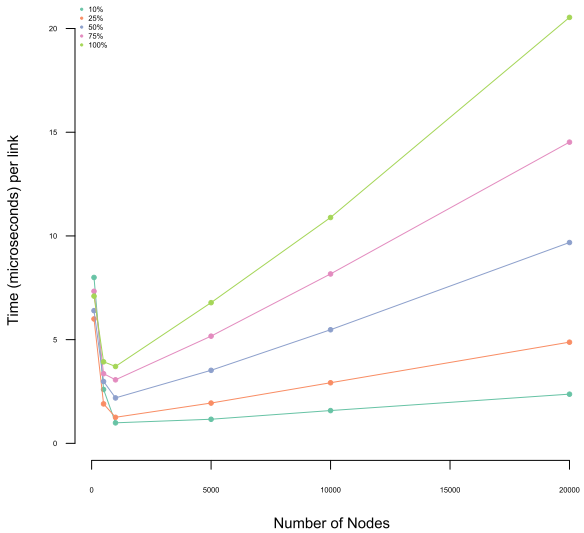

Fig. 3 Computational time for the calculation of `wTO` for each link for different sizes of networks and proportions of sets of nodes of interest: The run time of the *wTO* calculation increases with increasing proportion of nodes of interest. The graph presented here shows the time for computing each link for different sizes of nodes and proportions of subsets of nodes of interest

Comparison with existing methods

A variety of methods currently exist to analyze gene co-expression networks, in particular `ARACNe` [16, 17], SPACE [28] and `WGCNA` [14, 15]. These methods rest on a multitude of different mathematical principles, particularly with respect to how co-expression is quantified. Of particular interest is `WGCNA`, which shares notable similarities with our `wTO` package in heuristic terms, but with some substantial differences in functionality. In particular, `WGCNA` also uses the weighted topological overlap (in their nomenclature, the "topological overlap matrix", or TOM) to quantify co-expression at the gene-pair level. But in `WGCNA`, the final edge weight corresponds to the absolute value of $\omega_{i,j}$ as defined in Eq. 2, or the absolute value of the terms in the numerator of Eq. 2. These are referred to as signed or unsigned, respectively. Topological overlap as a measure of co-expression has previously been shown to compare favourably with other methods [18].

While `wTO` and `WGCNA` construct the networks based on overlaping topologies, the `ARACNe` method builds the network using the mutual information (MI) and removing links that are indirect interactions using data processing inequality (DPI). Another important difference between the methods is that `wTO` and `WGCNA` will compute a link for all pair-wise possible connections, while `ARACNe` will only compute the pair-wise information if their information is not independent (Table 1).

Relative to WGCNA, wTO provides three major additions: the determination of p-values (determined by bootstrapping) for each pairwise wTO value; the calculation of a consensus network, and the ability to visualize the topological overlap network (along with node grouping according to a choice of nine algorithms). While WGCNA provides a variety of tools for visualizing the hierarchical tree forming the network, as well as for rendering the correlation matrix in heatmap form, it does not provide a node-and-edge type view of the co-expression network (but does allow for exporting networks into Cytoscape, in which network views are possible). Additionally, the consensus network as defined in Eq. 6 differs from the consensus TOM defined in WGCNA, which simply assigns to each edge of the consensus network the minimal value of the topological overlap across the input conditions. This is a strict version of consensus (unanimity), in that it will discard any gene pair if the overlap is weak in even a single network. In contrast, while Eq. 6 will remove contributions from networks where the topological overlap is weak (or where the sign of the wTO score is in conflict with the other networks), an edge may still be included if it is sufficiently present across the other networks.

Further additions in wTO include the possibility of choosing the Spearman correlation as the basis of $a_{i,j}$ (while WGCNA provides biweight midcorrelation, or bicor for short; both provide Pearson), as well as reducing computation time by the option of restricting the calculation of wTO scores to a set of genes of interest (while still including the adjacency to genes outside this set in each inter-set wTO score).

Another minor difference resides in how wTO is determined for each gene with itself. From Eq. 2, we see that (assuming $a_{i,i} = 0$ and $a_{i,j} = a_{j,i}$):

$$\omega_{i,i} = \frac{\sum_{u=1}^{N} a_{i,u}a_{u,i} + a_{i,i}}{k_i + 1 - |a_{i,i}|} = \frac{\sum_{u=1}^{N} a_{i,u}^2}{\sum_{u=1}^{N} a_{i,u} + 1}. \quad (7)$$

For an unweighted network, where $a_{i,j} = 0$ or $a_{i,j} = 1$ for all (i, j), this approximates to $\omega_{i_i} \approx 1$ for large k_i. However, this is not the case for weighted networks. WGCNA differs from the wTO package in that $w_{i,i} = 1$ is explicitly set for all i, while our package retains the score as defined by Eq. 2.

Comparing wTO, WGCNA and ARACNe using an *E. coli* transcription factor network

In order to quantitatively compare the performance of wTO, WGCNA and ARACNe, we downloaded a gene expression dataset from *E. coli* from http://systemsbiology.ucsd.edu/InSilicoOrganisms/Ecoli/EcoliExpression2 [29–32]. The data consists of 213 Affymetrix microarray gene expression profiles, corresponding to multiple different strains under different growth conditions, and contains gene expression data for 7312 distinct probes. Gene expressions were calculated as the mean of probes corresponding to the same gene. To assess the capability of the three tools in identifying true TF-TF interactions, we used the RegulonDB [33] database, which contains experimental data from *E. coli*, as a reference. We defined as True-Positive interactions those that are described in RegulonDB, and as True-Negatives all interactions that could not be experimentally validated in that dataset. For comparison, we also calculated networks using only the raw Pearson correlation. We generated the network for WGCNA following the steps described by the authors in the Tutorial [11, 34]. We used the functions `pickSoftThreshold` and `pickHardThreshold` for defining the power of the soft-threshold and for choosing the hard-threshold, respectively. The power was defined as 4 and the hard-threshold was set to 0.3.

The ARACNe network was built using the Pearson correlation with `build.mim` and ARACNe functions in the `minet` R package [35]. The wTO networks were built using 1000 simulations, Pearson correlation and filtered for p_{adj}-values $\leq$0.01 and the 90% quantile. One wTO network was constructed using a δ of 0.2, the default of the `package`, and another network was built using a δ of 0.1. All networks were filtered to only contain TFs with information in the RegulonDB. We calculated the Receiver operating characteristic (ROC)-curve using the pROC R package [36] (see Fig. 4).

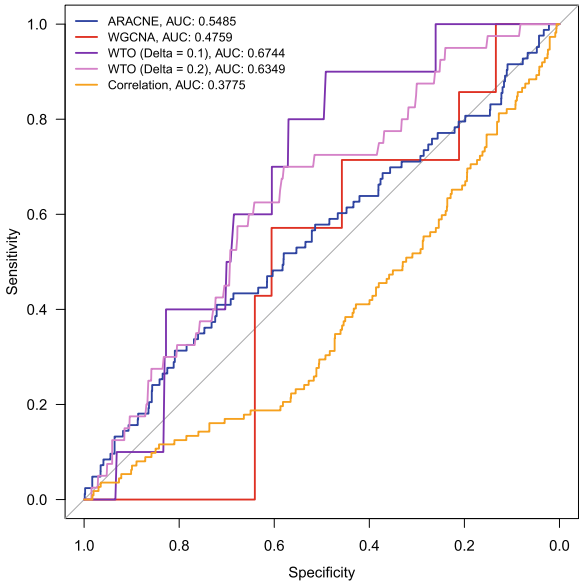

Fig. 4 ROC curves for the comparison of methods. Overall, our wTO method performs better than ARACNe, WGCNA and raw Pearson correlations. ARACNe is better in finding true positives, while WGCNA is more conservative, and therefore better in finding true negatives but identifies fewer true positives

Table 1 Comparison of key differences between wTO, `WGCNA` and `ARACNe`

Method	wTO	WGCNA	ARACNe
Topological overlap	Yes	Yes	No
Signed topological overlap	Optional	No	No
Consensus topological overlap	Weighted sum	Minimum weight (strict)	No
Pairwise *p*-values	Yes	No	Used to filter MI
Network view	Native	Exported to Cytoscape	Exported to Cytoscape
Soft thresholding	No	Optional (on by default)	No
Correlation choices	Spearman, Pearson	Bicor, Pearson	Spearman, Pearson, Kendall
Able to deal with time-series	Yes	No	No

`ARACNe` was able to better identify the amount of true positives compared to `WGCNA` and `wTO`, but performs worse when finding true negatives and also has a larger number of false positives (Fig. 4, Table 2). `WGCNA` is better at finding true negatives, but does not identify many true links. Our proposed *wTO* method performs better than `WGCNA` in finding true positives and better than `ARACNe` in finding true negatives. It also finds fewer false positives than `ARACNe`. In general, even when using a large δ, wTO performs better than the two other methods, as seen in the Area Under the Curve (AUC; the closer it is to unity, the better). This demonstrates that the use of the *wTO* method further reduces false effects coming from incorrectly assigned linked genes (false positives) when compared to ARACNe and raw correlations.

Examples of wTO networks using the wTO R package

wTO and CN networks for TFs of the human prefrontal cortex

To exemplify the usage and results of our package, we analyzed three independent datasets of microarray data from human prefrontal cortex. Data sets were downloaded as raw data from Gene Expression Omnibus (GEO) website [37]. From the study GSE20168 [38, 39], we used data from a total of 15 postmortem brain samples. From the study GSE2164 [40], we used a total of 26 samples from post mortem brains. And finally, from the study GSE54568 [41] we used all the 15 controls. All individuals were older than 5 years and died without any neuropathological phenotypes. We chose the TFs to be our genes of interest and calculated a TF-wTO network for each of the three datasets. Subsequently, we computed the consensus network for the three TF wTO networks.

The downloaded data were pre-processed and normalized by ourselves independently, using the `R` environment [42], and the `affy` [43] package from the `Bioconductor` set. The probe expression levels (RMA expression values) and MAS5 detection *p*-values were computed, and only probesets significantly detected in at least one sample (p-value <0.05) were considered. After the Quality Control and normalization of the data, the probes that were not specific for only one gene were deleted. If one gene was bound by more than one probeset, the average expression was computed.

Here, we will focus on how TFs are co-expressed in brain networks. We used a set of 3229 unique TF symbols from the TF-Catalog (*Perdomo-Sabogal* et al. *(in preparation)*) with ENSEMBL protein IDs. The construction of this catalog contains the information for TF proteins sourced from the most influential studies in the field of human Gene Regulatory Factors (GRF) inventories [44–51] that are associated with gene ontology terms for regulation of transcription, DNA-depending transcription, RNA polymerase II transcription co-factor and co-repressor activity, chromatin binding, modification, remodeling, or silencing, among others.

Signed wTO networks were calculated for each dataset separately using the function `wTO.Complete` of our `wTO R` package and then merged with the function `wTO.Consensus` into the consensus. Significance of all networks was evaluated using 1000 bootstraps, Pearson correlation and filtered for p_{adj}-value of < 0.01. The Consensus Network was built based on the calculated signed wTO values of significant links. Weights for links with in-significant wTO were set to zero. Figure 5

Table 2 Accuracy of the 3 methods and correlation

	ReactomeDB (Total)	Pearson correlation	ARACNe	WGCNA	wTO (delta 0.1)	wTO (delta 0.2)
True negative	7234	2259	2633	7092	6520	5235
False negative	0	216	245	321	318	288
False positive	0	4975	4601	142	714	1999
True positive	328	112	83	7	10	40
Total	7562	7562	7562	7562	7562	7562

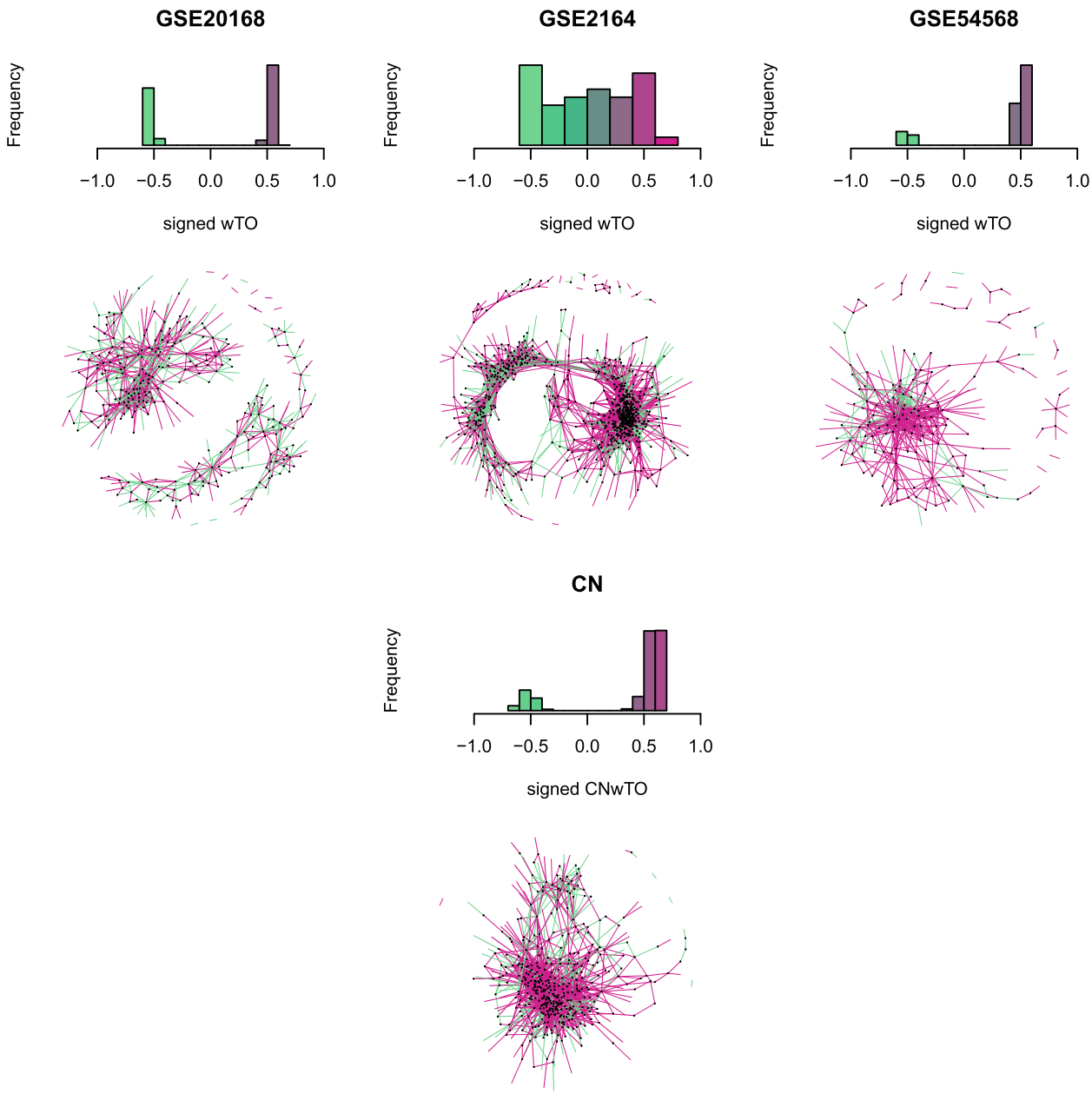

Fig. 5 Comparison of the three networks used to compute the CN. The first row shows the distribution of significant wTO values (p_{adj}-value < 0.01). Note that the wTO range of the second network is larger than of the other two networks. The second row show the wTO network for each method. The third and forth row refer to the CN. Note that now the distribution of the wTO values does not include the wTO values close to zero, and retains only values that show a high correlation between the TFs. In the histograms, the presence of negative wTO values is visible, indicating that there are TFs that downregulate other genes

shows the distributions and the networks for our three datasets.

TFs were clustered using the Louvain algorithm with the `NetVis` function, which identified 5 clusters in the CN. When considering each network independently, we had 18, 8 and 16 clusters. This shows that the CN detects fewer clusters of genes, which are more densely connected, compared to the clusters detected in the individual wTO networks. In order to investigate the function of each one of the 5 CN clusters, we calculated the correlation of each TF of a cluster with all other expressed genes using Pearson correlation. Genes with a correlation of at least |0.80| with at least one TF of the cluster were used for GO enrichment analysis for that cluster, using the R package `topGO` [52]. The enrichment analysis revealed many brain related functions, for instance, clusters 1 and

Table 3 GO terms associated with each one of the CN Clusters

Cluster	# TFs	Genes correlated to TFs	GO.ID	Term
1	589	58	GO:0042775	mitochondrial ATP synthesis coupled
			GO:0010498	proteasomal protein catabolic process
			GO:0050890	cognition
			GO:0033238	regulation of cellular amine metabolic pathway
			GO:0008090	retrograde axonal transport
			GO:0070050	neuron cellular homeostasis
			GO:0090168	Golgi reassembly
			GO:0006099	tricarboxylic acid cycle
			GO:0051443	positive regulation of ubiquitin-protein
			GO:0061418	regulation of transcription from RNA polimerase
			GO:0047496	vesicle transport along microtubule
			GO:0061640	cytoskeleton-dependent cytokinesis
			GO:0043488	regulation of mRNA stability
			GO:0000086	G2/M transition of mitotic cell cycle
			GO:0038061	NIK/NF-kappaB signaling
			GO:0000209	protein polyubiquitination
			GO:0007052	mitotic spindle organization
			GO:0031333	negative regulation of protein complex
			GO:0002223	stimulatory C-type lectin receptor signal
			GO:0016486	peptide hormone processing
			GO:0034314	Arp2/3 complex-mediated actin nucleation
			GO:1900271	regulation of long-term synaptic potential
			GO:0000715	nucleotide-excision repair, DNA damage
			GO:1901983	regulation of protein acetylation
			GO:0016082	synaptic vesicle priming
			GO:0043243	positive regulation of protein complex
			GO:2000637	positive regulation of gene silencing
			GO:0021902	commitment of neuronal cell
			GO:0051683	establishment of Golgi localization
			GO:0060013	righting reflex
			GO:0061732	mitochondrial acetyl-CoA biosynthetic pr...
2	647	77	GO:0035773	insulin secretion involved in cellular
			GO:0098930	axonal transport
			GO:0000086	G2/M transition of mitotic cell cycle
			GO:0061640	cytoskeleton-dependent cytokinesis
			GO:0090083	regulation of inclusion body assembly
			GO:0034112	positive regulation of homotypic
			GO:1902750	negative regulation of cell cycle G2/M
			GO:0031146	SCF-dependent proteasomal ubiquitin-dependent
			GO:0061003	positive regulation of dendritic spine
			GO:0032922	circadian regulation of gene expression
			GO:0072600	establishment of protein localization
			GO:0061077	chaperone-mediated protein folding
			GO:0016191	synaptic vesicle uncoating
			GO:1902309	negative regulation of peptidyl-serine
			GO:0048024	regulation of mRNA splicing, via spliceosome
			GO:0016486	peptide hormone processing
			GO:0048268	clathrin coat assembly
			GO:0000209	protein polyubiquitination
			GO:0035902	response to immobilization stress
			GO:2000757	negative regulation of peptidyl-lysine
3	40	17	GO:0043687	post-translational protein modification
			GO:0050851	antigen receptor-mediated signaling pathway
			GO:0002479	antigen processing and presentation
			GO:0090199	regulation of release of cytochrome c
			GO:1905323	telomerase holoenzyme complex assembly
			GO:0050890	cognition
			GO:0043248	proteasome assembly
			GO:0030177	positive regulation of Wnt
			GO:0030177	signaling pat...
			GO:0047496	vesicle transport along microtubule
			GO:0042775	mitochondrial ATP synthesis
			GO:0035773	insulin secretion involved in cellular
			GO:0045116	protein neddylation
			GO:0090141	positive regulation of mitochondrial
			GO:0060071	Wnt signaling pathway, planar cell
			GO:0010635	regulation of mitochondrial fusion
			GO:0016579	protein deubiquitination
			GO:0090090	negative regulation of canonical Wnt signal
			GO:0051131	chaperone-mediated protein complex
			GO:0051560	mitochondrial calcium ion homeostasis
			GO:0008090	retrograde axonal transport
			GO:0032700	negative regulation of interleukin-17
			GO:0048170	positive regulation of
			GO:0048170	long-term neuronal
			GO:0051036	regulation of endosome size
			GO:0061588	calcium activated phospholipid
			GO:0090149	mitochondrial membrane fission
			GO:0097112	gamma-aminobutyric acid receptor
			GO:0097332	response to antipsychotic drug
			GO:0097338	response to clozapine
			GO:1902683	regulation of receptor localization
			GO:0060052	neurofilament cytoskeleton organization
			GO:0048678	response to axon injury

Table 3 GO terms associated with each one of the CN Clusters *(Continued)*

Cluster	# TFs	Genes correlated to TFs	GO.ID	Term
4	677	39	GO:0007612	learning
			GO:0000209	protein polyubiquitination
			GO:0070646	protein modification by small protein
			GO:0035567	non-canonical Wnt signaling pathway
			GO:0038061	NIK/NF-kappaB signaling
			GO:0090313	regulation of protein targeting to membrane
			GO:0016339	calcium-dependent cell-cell adhesion
			GO:0002223	stimulatory C-type lectin receptor signal
			GO:0043687	post-translational protein modification
			GO:0008090	retrograde axonal transport
			GO:0061732	mitochondrial acetyl-CoA biosynthetic
			GO:0070050	neuron cellular homeostasis
			GO:0016236	macroautophagy
			GO:0043488	regulation of mRNA stability
			GO:0061178	regulation of insulin secretion involved...
			GO:0016486	peptide hormone processing
			GO:0035493	SNARE complex assembly
			GO:0034112	positive regulation of homotypic
			GO:1902260	negative regulation of delayed rectifier...
			GO:1902267	regulation of polyamine transmembrane
			GO:2000574	regulation of microtubule motor activity
			GO:0016082	synaptic vesicle priming
			GO:0051560	mitochondrial calcium ion homeostasis
			GO:0006596	polyamine biosynthetic process
			GO:0060052	neurofilament cytoskeleton organization
			GO:1903608	protein localization to cytoplasmic stress
			GO:0000715	nucleotide-excision repair, DNA damage
			GO:0047496	vesicle transport along microtubule
			GO:1990542	mitochondrial transmembrane transport
			GO:0031333	negative regulation of protein complex
			GO:0046826	negative regulation of protein export
5	18	4	GO:0072369	regulation of lipid transport
			GO:1901379	regulation of potassium ion transmembrane
			GO:0032700	negative regulation of interleukin-17
			GO:0051036	regulation of endosome size
			GO:1904219	positive regulation of CDP-diacylglycerol
			GO:1904222	positive regulation of serine C-palmitoyl
			GO:1905664	regulation of calcium ion import
			GO:2000286	receptor internalization
			GO:0021769	orbitofrontal cortex development
			GO:0045716	positive regulation of low-density lipo.
			GO:0060430	lung saccule development
			GO:0070885	negative regulation of calcineurin-NFAT
			GO:1900272	negative regulation of long-term synaptic
			GO:1902951	negative regulation of dendritic spine

3 show overrepresentation of groups related to cognition (Table 3 and Fig. 6).

Time series: Metagenomics data from the ocean

Only about 1% of marine bacteria can be easily studied using standard laboratory procedures [53]. This is a major drawback for the understanding of how those microorganisms interact. Systems biology methods can provide helpful insights to shed light on species interactions.

To demonstrate an application of our `wTO` package for time series data with no replicates, we use as an example metagenomics data from The USC Microbial Observatory. The data is public available at https://www.ebi.ac.uk/metagenomics/projects/ERP013549.

The sampling site is located between Los Angeles and the USC Wrigley Marine Laboratory on Santa Catalina and spans approximately 900 m of water. Over the course of 98 months, samples were taken once a month. Operational Taxonomic Unity (OTUs) were determined using 16S ribosomal RNA (rRNA). The authors found 67 OTUs that will be used in our analysis. In order to find the correct lag for the blocked bootstrap, we used the autocorrelation function (acf) for all OTUs and chose a median lag of 2. This allowed us to define the blocks with high autocorrelation in the same sample, meaning

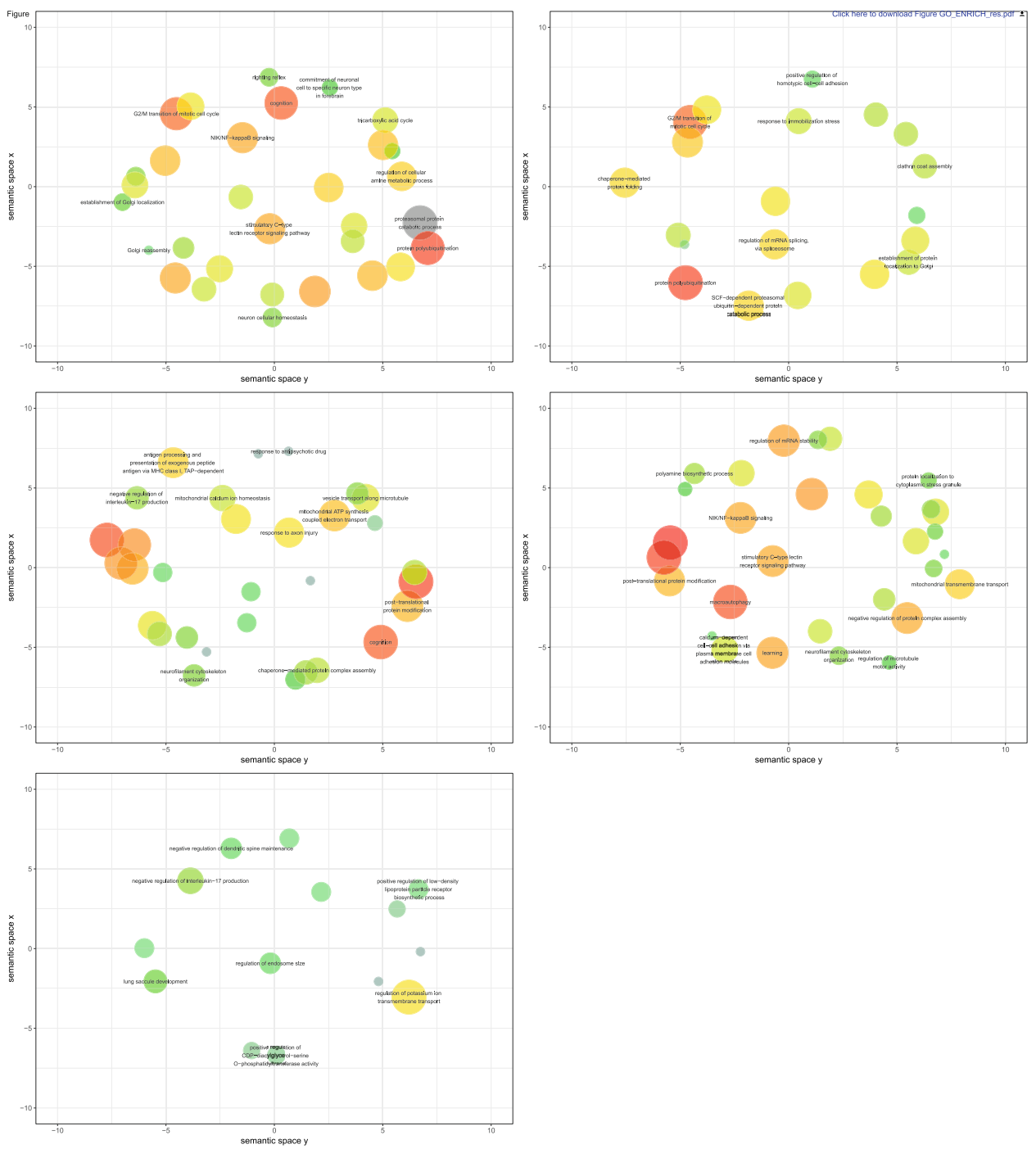

Fig. 6 GO terms enriched within each cluster. Enriched GO terms of the category "biological process" are clustered by REVIGO [76] with the SimRel measurement and allowed similarity of 0.5. The size of the circle represents the frequency of the GO term in the database, i.e. GO groups with many members are represented by larger circles. The color code refers to the $\log_{10}(p\text{-value})$ of the GO enrichment analysis: the closer to 0, the more red, the lower this value, the greener the bubble is. After removing redundancies, the remaining terms are visualized in *semantic similarity-based* scatter-plots, where the axes correspond to semantic distance. Brain related functions were detected, for instance in Clusters 1 and 3, that are involved with cognition

that for them the abundance of the OTU on each specific time point is correlated to the following next 2 time points.

Based on that, we built the network of bacteria co-occurrence in that environment (Fig. 7). We found that 61 out of 67 OTUs had at least one significant

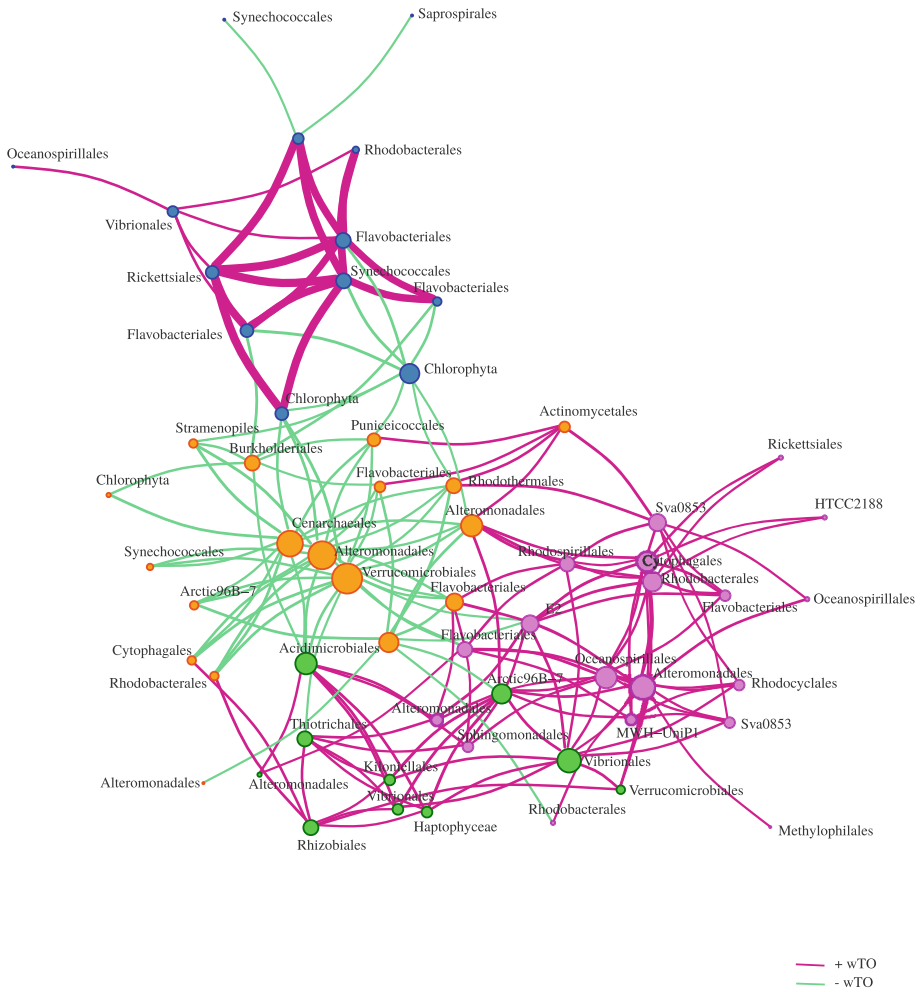

Fig. 7 OTUs analysis using the Time-Series method of the `wTO` package. In this network, the sizes of the nodes are proportional to a node's degree, and the width of a link is proportional to its wTO-absolute value. The link color refers to its sign, with green links being negative and purple ones positive. Nodes belonging to the same cluster are shown in the same color. There are four distinct clusters of bacteria. The orange cluster contains only negative interactions (green links), suggesting that the bacterial species in this cluster do not co-exist. We also notice, that many of the bacteria belonging to the same order are well connected by purple links, indicating that they co-exist and share interactions. However, the number of interactions among non-related bacteria demonstrate that interactions are not intra-order specific

interaction (p_{adj}-value < 0.01). Positive correlations in co-occurence networks may represent symbiotic or commensal relationships, while negative correlations may represent predator-prey interactions, allelopathy or competition for limited resources. Using the community detection method for defining clusters we identified four distinct clusters of bacteria. We did not find any association of the phylogeny with clusters, which is in agreement with previous studies. However, we can clearly see (Fig. 7) that the blue group is rich in negative relationships, while both, the purple and orange groups, possess many positive relationships. These positive relationships are formed mostly by Flavobacteriales, bacteria that are known to infect fishes [54] and to live in commensality with other bacteria from the same order [55].

Conclusion

This new `wTO` package allows *wTO* network calculation for both, positive and negative correlations, which is not provided in any other published `R` package. With this feature it becomes valuable for the analysis of gene regulatory network, metabolic networks, ecological networks and other networks, in which the biological interpretation strongly depends on distinguishing between activating and inhibiting/repressing interactions.

Another novel feature is the computation of *p*-values for each link based on its empirical distribution, which allows for the reduction of false positive links in wTO networks. With our package, networks can also be calculated from time series data. In addition, our package includes the computation of a *CN*, which enables integrating

networks derived from different studies or datasets to determine links that consistently appear in these networks.

By focusing on what these independently derived networks have in common, the CN should be of higher biological confidence than each individual network is. We also provide an interactive visualization tool that can be used to visualize both, *wTO* networks and *CN*, for efficient further custom analysis.

We qualitatively and quantitatively compared our new package to state-of-the-art methods and demonstrated that it performs better in identifying true positives and false negatives.

We provide two use cases for our package, one on wTO and CN calculation from three independent genome-wide expression datasets of human pre-frontal cortex samples, and one on wTO co-occurence networks calculated from time series data of a metagenomics abundance dataset from the ocean. Here, we demonstrated that clusters and GO enrichment in the CN are more defined than in individual wTO networks, highlighting the benefits of our package for analyzing and interpreting large biological datasets.

Availability and requirements

Project name: wTO: Computing Weighted Topological Overlaps (wTO) & Consensus wTO Network
Project home page: https://CRAN.R-project.org/package=wTO
Operating system: Platform independent
Programming language: R
Other requirements: `wTO` relies on the following packages: `som` [56], `plyr` [57], `stringr` [58], `network` [59, 60], `igraph` [27], `visNetwork` [61], `data.table` [62] and the standard packages `stats` and `parallel` [25]. The visualization tool implemented in our package was built using a combination of the packages `network` [59, 60], `igraph` [27] and `visNetwork` [61]. The `MakeGroups` parameter, passed to the function `NetVis` for constructing the network, allows the user to choose clustering algorithms from: "walktrap" [63], "optimal"[64], "spinglass" [65–67], "edge.betweenness' [68, 69], 'fast_greedy" [70], "infomap' [71, 72], "louvain" [73], "label_prop' [74] and "leading_eigen" [75]. All those algorithms are implemented in the `igraph` package[27].
License: GLP-2

Abbreviations

acf: Autocorrelation function; ARACNe: An algorithm for the reconstruction of gene regulatory networks; AUC: Area under the curve; CN: Consensus network; DPI: data processing inequality; GEO: Gene expression Omnibus; MI: Mutual information; miRNA: Micro RNA; ncRNA: Non coding RNA; OTU: Operational taxonomic unit; PFC: Pre-frontal cortex; ROC: Receiver operating characteristic; TF: Transcription factor; TOM: Topological overlap matrix; WGCNA: Weighted correlation network analysis; wTO: Weighted topological overlap

Acknowledgements

We thank Professor Martin Middendorf, Martina Hall and Marlis Reich for fruitful discussions on the methodology and suggestions on the package. We thank Alvaro Perdomo Sabogal for providing us the Transcription Factors list used to build the PFC networks. We thank Daniel Gerighausen for discussions. We acknowledge support by the German Research Foundation and the Open Access Publication Fund of the Freie Universität Berlin.

Funding

This work was supported partially by a doctoral grant from the Brazilian government's Science without Borders program (GDE 204111/2014-5).

Availability of data and materials

`wTO` is open source and freely available from `CRAN` https://cran.r-project.org/web/packages/wTO/ under the the GPL-2 Open Source License. It is platform independent.

Authors' contributions

DG implemented the code in R. DG and TM conceived the idea of *p*-values for the edges. KN and EA generalized the *wTO* for signed values. DG and AV compared the wTO method to other methods. DG run the example analysis. DG wrote the draft of manuscript. All authors discussed the manuscript, read and approved the final version of the manuscript.

Ethics approval and consent to participate

Not applicable.

Consent for publication

Not applicable.

Competing interests

The authors declare that they have no competing interests.

Publisher's Note

Author details

[1]Department of Computer Science, Interdisciplinary Center of Bioinformatics, University of Leipzig, Haertelstrasse 16-18, 04109 Leipzig, Germany. [2]Swarm Intelligence and Complex Systems Group, Faculty of Mathematics and Computer Science, University of Leipzig, Augustusplatz 10, 04109 Leipzig, Germany. [3]Department of Biotechnology, NTNU - Norwegian University of Science and Technology, N-7049 Trondheim, Norway. [4]Fundação Cesgranrio, Rio de Janeiro, 20261-903 Rio de Janeiro, Brazil. [5]K.G. Jebsen Center for Genetic Epidemiology, Department of Public Health, NTNU - Norwegian University of Science and Technology, N-7049 Trondheim, Norway. [6]Freie Universität Berlin, Human Biology Group, Institute for Zoology, Department of Biology, Chemistry and Pharmacy, Königin-Luise-Straße 1-3, D-14195 Berlin, Germany.

Received: 23 November 2017 Accepted: 30 August 2018
Published online: 24 October 2018

References

1. Barabasi A-L, Oltvai ZN. Network biology: understanding the cell's functional organization. Nat Rev Genet. 2004;5(2):101–13.
2. Bansal M, Belcastro V, Ambesi-Impiombato A, Di Bernardo D. How to infer gene networks from expression profiles. Mol Syst Biol. 2007;3(1):78.
3. Furlong LI. Human diseases through the lens of network biology. Trends Genet. 2013;29(3):150–59.
4. Dempsey K, Thapa I, Cortes C, Eriksen Z, Bastola DK, Ali H. On Mining Biological Signals Using Correlation Networks. In: 2013 IEEE 13th International Conference on Data Mining Workshops; 2013. p. 327–334. https://doi.org/10.1109/ICDMW.2013.125.
5. Yang Y, Han L, Yuan Y, Li J, Hei N, Liang H. Gene co-expression network analysis reveals common system-level properties of prognostic genes across cancer types. Nat Commun. 2014;5:3231.
6. Taylor IW, Linding R, Warde-Farley D, Liu Y, Pesquita C, Faria D, Bull S, Pawson T, Morris Q, Wrana JL. Dynamic modularity in protein interaction networks predicts breast cancer outcome. Nat Biotechnol. 2009;27(2):199–04.
7. van Dam S, Võsa U, van der Graaf A, Franke L, de Magalhães JP. Gene co-expression analysis for functional classification and gene–disease predictions. Brief Bioinform. 2017;139.

8. Babu MM, Luscombe NM, Aravind L, Gerstein M, Teichmann SA. Structure and evolution of transcriptional regulatory networks. Curr Opin Struct Biol. 2004;14(3):283–91.
9. Mason MJ, Fan G, Plath K, Zhou Q, Horvath S. Signed weighted gene co-expression network analysis of transcriptional regulation in murine embryonic stem cells. BMC genomics. 2009;10(1):327.
10. Ravasz E, Somera AL, Mongru DA, Oltvai ZN, Barabási A-L. Hierarchical organization of modularity in metabolic networks. Science. 2002;297(5586):1551–55.
11. Zhang B, Horvath S. A general framework for weighted gene co-expression network analysis. Stat Appl Genet Mol Biol. 2005;4:17.
12. Carlson MR, Zhang B, Fang Z, Mischel PS, Horvath S, Nelson SF. Gene connectivity, function, and sequence conservation: predictions from modular yeast co-expression networks. BMC Genomics. 2006;7(1):40.
13. Nowick K, Gernat T, Almaas E, Stubbs L. Differences in human and chimpanzee gene expression patterns define an evolving network of transcription factors in brain. Proc Natl Acad Sci. 2009;106(52):22358–363.
14. Langfelder P, Horvath S. Wgcna: an r package for weighted correlation network analysis. BMC Bioinf. 2008;9(1):559.
15. Langfelder P, Horvath S. Fast R functions for robust correlations and hierarchical clustering. J Stat Softw. 2012;46(11):1–17.
16. Margolin AA, Wang K, Lim WK, Kustagi M, Nemenman I, Califano A. Reverse engineering cellular networks. Nat Protoc. 2006;1(2):662.
17. Margolin AA, Nemenman I, Basso K, Wiggins C, Stolovitzky G, Dalla Favera R, Califano A. ARACNE: an algorithm for the reconstruction of gene regulatory networks in a mammalian cellular context. BMC Bioinf. 2006;7(Suppl 1):S7.
18. Allen JD, Xie Y, Chen M, Girard L, Xiao G. Comparing statistical methods for constructing large scale gene networks. PLoS ONE. 2012;7(1):1–9. https://doi.org/10.1371/journal.pone.0029348.
19. Berto S, Perdomo-Sabogal A, Gerighausen D, Qin J, Nowick K. A consensus network of gene regulatory factors in the human frontal lobe. Front Genet. 2016;7:31.
20. Efron B, Tibshirani RJ. An introduction to the bootstrap. Ed. Chapman & Hall. 1994;1:31–103. New York.
21. Altman DG. Practical statistics for medical research. 1990;624:277–321.
22. McCrum-Gardner E. Which is the correct statistical test to use? Br J Oral Maxillofac Surg. 2008;46(1):38–41.
23. Mukaka M. A guide to appropriate use of correlation coefficient in medical research. Malawi Med J. 2012;24(3):69–71.
24. Bishara AJ, Hittner JB. Testing the significance of a correlation with nonnormal data: comparison of pearson, spearman, transformation, and resampling approaches. Psychol Methods. 2012;17(3):399.
25. R Core Team. R: A Language and Environment for Statistical Computing. Vienna, Austria: R Foundation for Statistical Computing; 2017. https://www.R-project.org/.
26. Shannon P, Markiel A, Ozier O, Baliga NS, Wang JT, Ramage D, Amin N, Schwikowski B, Ideker T. Cytoscape: a software environment for integrated models of biomolecular interaction networks. Genome Res. 2003;13(11):2498–04.
27. Csardi G, Nepusz T. The igraph software package for complex network research. Inter J, Complex Sys. 2006;1695(5):1–9.
28. Peng J, Wang P, Zhou N, Zhu J. Partial correlation estimation by joint sparse regression models. J Am Stat Assoc. 2009;104(486):735–46. https://doi.org/10.1198/jasa.2009.0126.
29. Lewis NE, Cho B-K, Knight EM, Palsson BO. Gene Expression Profiling and the Use of Genome-Scale In Silico Models of Escherichia coli for Analysis: Providing Context for Content. J Bacteriol. 2009;191(11):3437–44. https://doi.org/10.1128/JB.00034-09.
30. Fong SS, Joyce AR, Palsson BO. Parallel adaptive evolution cultures of Escherichia coli lead to convergent growth phenotypes with different gene expression states. Genome Res. 2005;15(10):1365–72. https://doi.org/10.1101/gr.3832305.
31. Fong SS, Nanchen A, Palsson BO, Sauer U. Latent Pathway Activation and Increased Pathway Capacity Enable Escherichia coli Adaptation to Loss of Key Metabolic Enzymes. J Biol Chem. 2006;281(12):8024–33. https://doi.org/10.1074/jbc.M510016200.
32. Covert MW, Knight EM, Reed JL, Herrgard MJ, Palsson BO. Integrating high-throughput and computational data elucidates bacterial networks. Nature. 2004;429(6987):92–6. https://doi.org/10.1038/nature02456.
33. Gama-Castro S, Salgado H, Santos-Zavaleta A, Ledezma-Tejeida D, Muñiz-Rascado L, García-Sotelo JS, Alquicira-Hernández K, Martínez-Flores I, Pannier L, Castro-Mondragón JA, Medina-Rivera A, Solano-Lira H, Bonavides-Martínez C, Pérez-Rueda E, Alquicira-Hernández S, Porrón-Sotelo L, López-Fuentes A, Hernández-Koutoucheva A, Moral-Chávez VD, Rinaldi F, Collado-Vides J. RegulonDB version 9.0: high-level integration of gene regulation, coexpression, motif clustering and beyond. Nucleic Acids Res. 2016;44(D1):133–43. https://doi.org/10.1093/nar/gkv1156.
34. Horvath S, Zhang B, Carlson M, Lu KV, Zhu S, Felciano RM, Laurance MF, Zhao W, Qi S, Chen Z, Lee Y, Scheck AC, Liau LM, Wu H, Geschwind DH, Febbo PG, Kornblum HI, Cloughesy TF, Nelson SF, Mischel PS. Analysis of oncogenic signaling networks in glioblastoma identifies ASPM as a molecular target. Proc Natl Acad Sci. 2006;103(46):17402–07. https://doi.org/10.1073/pnas.0608396103.
35. Meyer PE, Lafitte F, Bontempi G. MINET: An open source R/Bioconductor Package for Mutual Information based Network Inference. BMC Bioinf. 2008;9. http://www.biomedcentral.com/1471-2105/9/461.
36. Robin X, Turck N, Hainard A, Tiberti N, Lisacek F, Sanchez J-C, Müller M. proc: an open-source package for r and s+ to analyze and compare roc curves. BMC Bioinf. 2011;12:77.
37. Edgar R, Domrachev M, Lash AE. Gene expression omnibus: Ncbi gene expression and hybridization array data repository. Nucleic acids res. 2002;30(1):207–10.
38. Zhang Y, James M, Middleton FA, Davis RL. Transcriptional analysis of multiple brain regions in parkinson's disease supports the involvement of specific protein processing, energy metabolism, and signaling pathways, and suggests novel disease mechanisms. Am J Med Genet B Neuropsychiatr Genet. 2005;137(1):5–16.
39. Zheng B, Liao Z, Locascio JJ, Lesniak KA, Roderick SS, Watt ML, Eklund AC, Zhang-James Y, Kim PD, Hauser MA, et al. Pgc-1α, a potential therapeutic target for early intervention in parkinson's disease. Sci Transl Med. 2010;2(52):52–735273.
40. Vawter MP, Evans S, Choudary P, Tomita H, Meador-Woodruff J, Molnar M, Li J, Lopez JF, Myers R, Cox D, et al. Gender-specific gene expression in post-mortem human brain: localization to sex chromosomes. Neuropsychopharmacology. 2004;29(2):373.
41. Chang L-C, Jamain S, Lin C-W, Rujescu D, Tseng GC, Sibille E. A conserved bdnf, glutamate-and gaba-enriched gene module related to human depression identified by coexpression meta-analysis and dna variant genome-wide association studies. PloS ONE. 2014;9(3):90980.
42. R Core Team. R: A Language and Environment for Statistical Computing. Vienna, Austria: R Foundation for Statistical Computing; 2017. https://www.R-project.org/.
43. Gautier L, Cope L, Bolstad BM, Irizarry RA. affy—analysis of affymetrix genechip data at the probe level. Bioinformatics. 2004;20(3):307–15. https://doi.org/10.1093/bioinformatics/btg405.
44. Messina DN, Glasscock J, Gish W, Lovett M. An orfeome-based analysis of human transcription factor genes and the construction of a microarray to interrogate their expression. Genome Res. 2004;14(10b):2041–47.
45. Vaquerizas JM, Kummerfeld SK, Teichmann SA, Luscombe NM. A census of human transcription factors: function, expression and evolution. Nat Rev Genet. 2009;10(4):252.
46. Ravasi T, Suzuki H, Cannistraci CV, Katayama S, Bajic VB, Tan K, Akalin A, Schmeier S, Kanamori-Katayama M, Bertin N, et al. An atlas of combinatorial transcriptional regulation in mouse and man. Cell. 2010;140(5):744–52.
47. Nowick K, Fields C, Gernat T, Caetano-Anolles D, Kholina N, Stubbs L. Gain, loss and divergence in primate zinc-finger genes: a rich resource for evolution of gene regulatory differences between species. PLoS ONE. 2011;6(6):21553.
48. Corsinotti A, Kapopoulou A, Gubelmann C, Imbeault M, de Sio FRS, Rowe HM, Mouscaz Y, Deplancke B, Trono D. Global and stage specific patterns of krüppel-associated-box zinc finger protein gene expression in murine early embryonic cells. PloS ONE. 2013;8(2):56721.
49. Tripathi S, Christie KR, Balakrishnan R, Huntley R, Hill DP, Thommesen L, Blake JA, Kuiper M, Lægreid A. Gene ontology annotation of sequence-specific dna binding transcription factors: setting the stage for a large-scale curation effort. Database. 2013;2013:062.
50. Wingender E, Schoeps T, Dönitz J. Tfclass: an expandable hierarchical classification of human transcription factors. Nucleic Acids Res. 2012;41(D1):165–70.
51. Wingender E, Schoeps T, Haubrock M, Dönitz J. Tfclass: a classification of human transcription factors and their rodent orthologs. Nucleic Acids Res. 2014;43(D1):97–02.

52. Alexa A, Rahnenführer J. Gene set enrichment analysis with topGO. Bioconductor Improv. 2009;27.
53. Mac Rygaard A, Thøgersen MS, Nielsen KF, Gram L, Bentzon-Tilia M. Effects of gelling agent and extracellular signaling molecules on the culturability of marine bacteria. Appl Environ Microbiol. 2017;83(9): 00243–17.
54. Loch TP, Faisal M. Emerging flavobacterial infections in fish: A review. J Adv Res. 2015;6(3):283–300. Editors and International Board Member collection.
55. Bernardet J-F. Bergey's Manual of Systematic Bacteriology, 2nd ed., vol. 1 (The Archaea and the deeply branching and phototrophic Bacteria) (D.R. Boone and R.W. Castenholz, eds.) New York: Springer-Verlag; 2001. pp. 465–466.
56. Yan J. Som: Self-Organizing Map. 2016. R package version 0.3-5.1. https://CRAN.R-project.org/package=som.
57. Wickham H. The split-apply-combine strategy for data analysis. J Stat Softw. 2011;40(1):1–29.
58. Wickham H. stringr: modern, consistent string processing. The R J. 2010;2(2):38–40.
59. Butts C. T. network: a package for managing relational data in r. J Stat Softw. 2008;24(2).
60. Butts CT. Network: Classes for Relational Data. 2015. The Statnet Project (http://statnet.org). R package version 1.13.0. http://CRAN.R-project.org/package=network.
61. Almende BV, Thieurmel B. visNetwork: Network Visualization Using 'vis.js' Library. 2016. R package version 1.0.3. https://CRAN.R-project.org/package=visNetwork.
62. Dowle M, Srinivasan A. Data table: Extension of data frame. 2017. R package version 1.10.4. https://CRAN.R-project.org/package=data.table.
63. Pons P, Latapy M. Computing communities in large networks using random walks. J Graph Algorithms Appl. 2006;10(2):191–18.
64. Brandes U, Delling D, Gaertler M, Gorke R, Hoefer M, Nikoloski Z, Wagner D. On modularity clustering. IEEE Trans Knowl Data Eng. 2008;20(2):172–88.
65. Reichardt J, Bornholdt S. Statistical mechanics of community detection. Physical Review E. 2006;74(1):016110.
66. Newman ME, Girvan M. Finding and evaluating community structure in networks. Physical Rev E. 2004;69(2):026113.
67. Traag VA, Bruggeman J. Community detection in networks with positive and negative links. Phys Rev E. 2009;80(3):036115.
68. Freeman LC. Centrality in social networks conceptual clarification. Soc Netw. 1978;1(3):215–39.
69. Brandes U. A faster algorithm for betweenness centrality. J Math Sociol. 2001;25(2):163–77.
70. Clauset A, Newman ME, Moore C. Finding community structure in very large networks. Phys Rev E. 2004;70(6):066111.
71. Rosvall M, Axelsson D, Bergstrom CT. The map equation. Eur Phys J Spec Top. 2009;178(1):13–23. https://doi.org/10.1140/epjst/e2010-01179-1. Springer.
72. Rosvall M, Axelsson D, Bergstrom CT. The map equation. Eur Phys J-Special Topics. 2009;178(1):13–23. Springer https://doi.org/10.1140/epjst/e2010-01179-1.
73. Blondel VD, Guillaume J-L, Lambiotte R, Lefebvre E. Fast unfolding of communities in large networks. J stat mech: theory and experiment. 2008;2008(10):10008.
74. Raghavan UN, Albert R, Kumara S. Near linear time algorithm to detect community structures in large-scale networks. Phys Rev E. 2007;76(3): 036106.
75. Newman ME. Finding community structure in networks using the eigenvectors of matrices. Phys Rev E. 2006;74(3):036104.